High Temperature Compressive Creep and Hot Hardness of Uranium-Plutonium Carbides

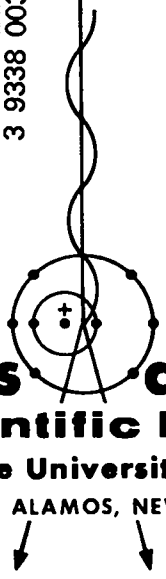

los alamos
scientific laboratory
of the University of California
LOS ALAMOS, NEW MEXICO 87544

UNITED STATES
ATOMIC ENERGY COMMISSION
CONTRACT W-7405-ENG. 36

Printed in the United States of America. Available from
National Technical Information Service
U. S. Department of Commerce
5285 Port Royal Road
Springfield, Virginia 22151
Price: Printed Copy $3.00; Microfiche $0.95

LA-4704
UC-25
ISSUED: July 1971

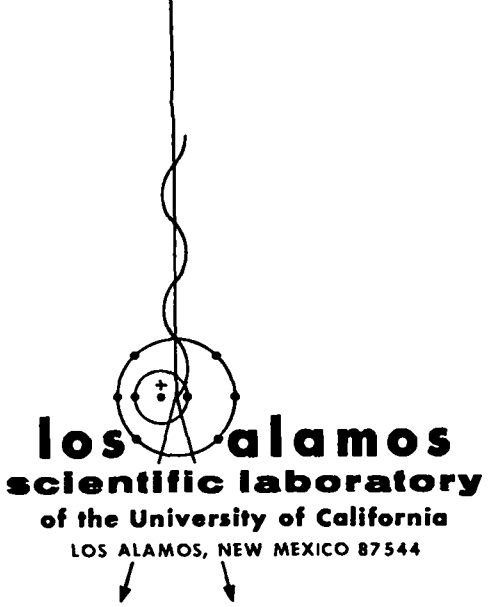

High Temperature Compressive Creep and Hot Hardness of Uranium-Plutonium Carbides

by

Michael Tokar

HIGH TEMPERATURE COMPRESSIVE CREEP AND HOT HARDNESS OF URANIUM - PLUTONIUM CARBIDES

by

Michael Tokar

ABSTRACT

The compressive creep of uranium-plutonium carbides having the composition $U_{0.79}Pu_{0.21}C_{1.02}$ and a sintered density of 11.8 g/cm^3 was studied at 1300, 1400, and 1500°C and stresses of 2000, 4000 and 6000 psi. The equation which best fitted the data was

$$\dot{\epsilon} = 7.96 \times 10^4 \sigma^{2.44} \exp\left(\frac{-126.4 \text{ kcal/mole}}{RT}\right).$$

The dominant creep mechanism was probably grain boundary sliding.

The hardness of some monocarbides with various U/Pu ratios was measured from room temperature to 1200°C. Probable mechanisms of deformation are discussed.

I. INTRODUCTION

As part of a programmatic study of the uranium-plutonium carbides as advanced fast reactor fuel materials, an investigation of some of their mechanical properties has been undertaken at the Los Alamos Scientific Laboratory (LASL). The principal goal of this investigation has been to determine the mechanical properties of well-characterized, relatively pure materials with special emphasis on determining the effect of microstructure, i.e., grain size, porosity, and secondary phases, on structure-sensitive properties such as high temperature creep. Since a knowledge of the mechanical properties of the fuel element material is a requisite for reactor design, this study has provided useful engineering data, and it is hoped that this information, coupled with elastic moduli measurements and diffusion data, might be used to enhance our understanding of basic high temperature deformation mechanisms in the actinide carbides.

II. COMPRESSIVE CREEP

A. Equipment and Procedure

$U_{0.79}Pu_{0.21}C_{1.02}$ creep specimens (spectrochemical analysis shown in Table I), having a sintered

TABLE I

SPECTROCHEMICAL ANALYSIS OF $U_{0.79}Pu_{0.21}C_{1.02}$ CREEP SPECIMEN MATERIAL*

Li	< 5	Ni	15
Be	< 1	Cu	< 2
B	< 1	Zn	< 10
Na	< 5	Sr	< 10
Mg	< 5	Zr	< 100
Al	< 10	Nb	< 100
Si	25	Mo	< 10
Ca	< 5	Cd	< 10
V	< 5	Sn	< 5
Cr	< 10	Ta	< 1000
Mn	< 5	W	40
Fe	75	Pb	< 5
Co	< 10	Bi	< 2

* In ppm.

density* of about 11.8 g/cm^3, were creep tested at 1300, 1400, and 1500°C under compressive stresses of 2000, 4000, and 6000 psi. A schematic diagram of the creep apparatus is shown in Fig. 1. In this apparatus, solid cylindrical specimens approximately 0.5 in. long and 0.4 in. in diam are heated in a graphite susceptor and compressed between two graphite rods. The load is applied hydraulically by a ram which passes through the glovebox floor and furnace chamber bottom plate. The graphite susceptor rests on a stack of pyrolytic graphite insulating disks atop the hydraulic ram. Changes in stoichiometry in the specimens due to carbon pick-up from the graphite push-rods are reduced by 30-mil-thick boron carbide disks which are placed between the ends of the specimen and the graphite rods. The assembly is completed by a stack of pyrolytic graphite disks placed above the top push-rod.

The creep data presented here were obtained from micrometer measurements of the specimen dimensions made before and after each creep run. Because of the limitations of this procedure, an optical extensometer has been set up and future measurements will be made with this instrument.

* Details of specimen preparation are given in "Synthesis and Fabrication of Pure, Single-Phase Uranium-Plutonium Monocarbide Pellets," by M.W. Shupe, A.E. Ogard, and J.A. Leary, Los Alamos Scientific Laboratory report LA-4283 (1969).

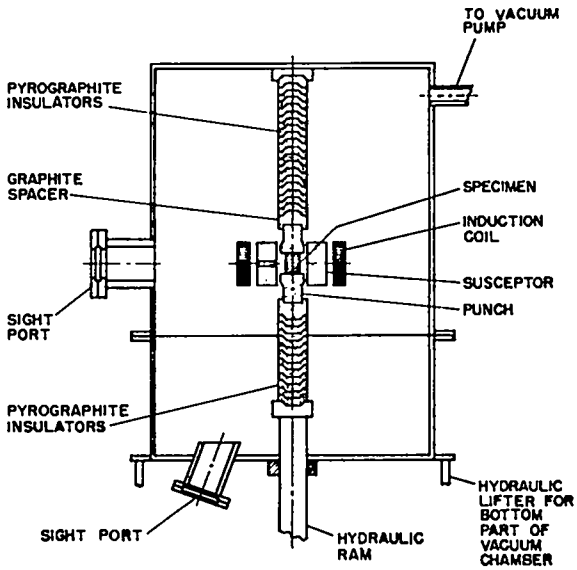

Fig. 1. Compressive creep apparatus.

Temperatures are measured optically by sighting through a hole in the susceptor on to the sample surface. The optical pyrometer was calibrated against a tungsten filament standard after interposing layers of glovebox window glass and quartz vacuum chamber window between the pyrometer and the standard.

B. Results

Some typical creep curves are shown in Fig. 2. The primary creep regions are extensive, but this may be partially attributed to the low initial density (~ 80% theoretical) of the specimens. Densification up to 92% of theoretical density was observed during the tests. Most of the density increase occurred before the onset of secondary creep. Secondary creep rates obtained from these data were fit by a least-squares method to an equation of the form

$$\dot{\epsilon} = A\sigma^n e^{-Q/RT}. \quad (1)$$

In Eq. (1), $\dot{\epsilon}$ is the creep rate (hours^{-1}), σ is the compressive stress (psi), R is the gas constant (kcal/mole/°K), T is the temperature (°K), Q is the activation energy (kcal/mole), n is the stress exponent, and A is a constant. The equation that best fit the data was

$$\dot{\epsilon} = 7.96 \times 10^4 \sigma^{2.44} \exp\left(\frac{-126.4 \text{ kcal/mole}}{RT}\right). \quad (2)$$

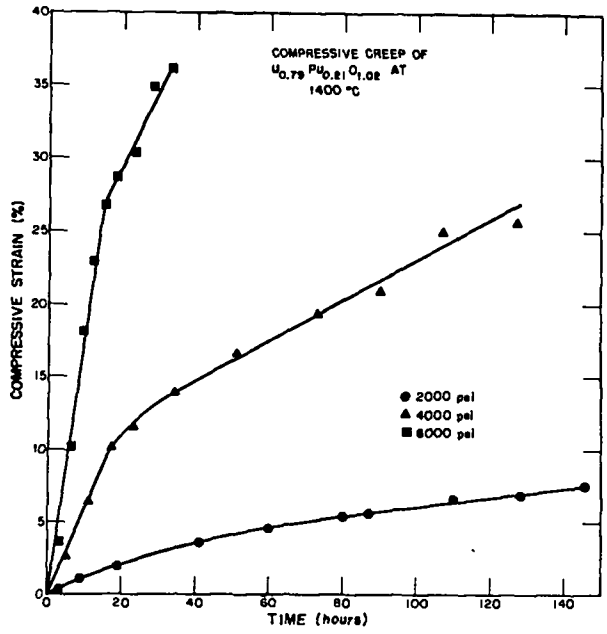

Fig. 2. Typical creep curves.

The standard deviations for the stress exponent and activation energy were 0.20 and 5.1 kcal/mole, respectively. Creep rates predicted by this equation were within 30% of experimentally determined values.

An Arrhenius plot of the secondary creep rates is shown in Fig. 3. The solid lines were calculated from Eq. (2). It is evident that the activation energy was independent of stress and temperature. The activation energy for creep of $(U_{0.85}Pu_{0.15})C_{0.65}N_{0.35}$ has been reported[1] as 100 ± 10 kcal/mole and, in a study of creep in UC and (U, Pu)C, Killey et al[2] reported an activation energy on the order of 100 kcal/mole for creep in $(U, Pu)C_{1-x}$ containing about 15% PuC in solid solution.

Other investigators[3-9] of creep in UC have reported activation energies between 37.5 and 90 kcal/mole. A compilation of the reported activation energies from some of these studies is given in Table II along with the results of some self-diffusion studies in UC.[10-17] The activation energy for high temperature creep for most metals and ceramics is found to be nearly equal to that for self-diffusion,[18] but in the case of UC it is difficult to interpret the mechanical behavior at high

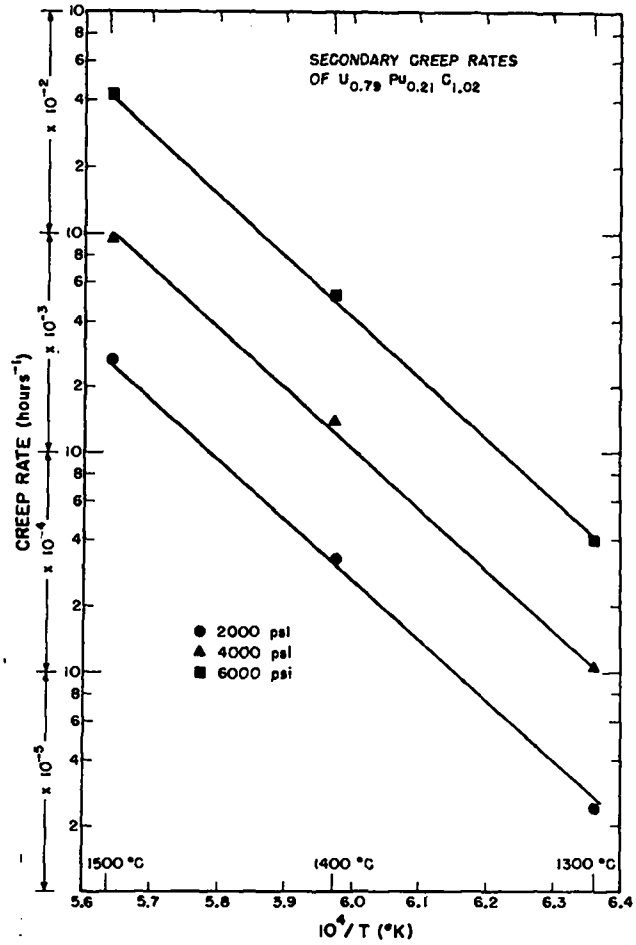

Fig. 3. Arrhenius plot.

temperatures in terms of the self-diffusion measurements due to the wide range of activation energies reported and also because the creep studies were not conducted on the same material used in the self-diffusion work. Most investigators agree that carbon diffuses 2 to 3 times faster than uranium in UC, hence one would assume that uranium diffusion is rate-controlling for creep. In some cases,[10, 13] however, evidence of enhanced grain boundary diffusion of uranium in limited temperature ranges has been reported, with resulting low values for the activation energy for self-diffusion. Until both creep and self-diffusion measurements are conducted at the same laboratory on the same material, the rate-controlling diffusion mechanism will remain in doubt. For the solid-solution uranium-plutonium carbides, no self-diffusion studies have been reported and

TABLE II

ACTIVATION ENERGIES FOR CREEP AND SELF-DIFFUSION IN UC

Reference	Temperature Range (°C)	% C	Q_{creep}	Q_U	Q_C
Nocreye (3)	1060-1500	4.8	48	—	—
Fassler et al. (4)	1100-1300	4.8	44	—	—
Stellrecht et al. (5)	1200-1400	5.2	90	—	—
Chang (8)	1500-1900	—	37.5	—	—
Kilby et al. (2)	1000-1350	4.84-5.4	70-250[a]	—	—
Beals & Ervin (18)	1100-2000	4.4 -4.8	—	32 - 150[b]	50 - 90[c]
Kratochwil (11)	1150-1494	~4.8	—	—	62.5
Wallace et al. (12)	1100-2400	~4.8	—	—	64
Lindner et al. (13)	800-2100	4.66-4.83	—	30[d] - 90[e]	—
Chubb et al. (14)	1400-2190	4.8 -5.1	—	65	58
Villaine & Marin (15)	1450-1968	4.63-5.8	—	86	—
Lee & Harrell (16)	1500-1900	≤4.82	—	104	62
Accary & Trouve (17)	700-1000	≤4.8	—	72	—

a. Q varied with temperature with a maximum at ~1150°C.
b. Q = 32 kcal/mole below 1700°C, 150 kcal/mole above 1700°C for stoichiometric and hypostoichiometric material, and 70 kcal/mole for hyperstoichiometric.
c. Q = 50 kcal/mole below 1500°C, and 90 kcal/mole above 1500°C.
d. 30 kcal/mole for 4.65% material up to 1400°C, then 70 kcal/mole.
e. 90 kcal/mole for 4.83% material above 1400°C.

so no attempt to analyse the creep measurements in terms of diffusion data can be made.

Although the activation energies for creep and self-diffusion have not been very useful in interpreting the creep behavior, an analysis of the effect of stress on creep rate may be more helpful in this regard. The effect of stress on secondary creep rate in $U_{0.79}Pu_{0.21}C_{1.02}$ is illustrated in Fig. 4. The value of the stress exponent, n, is of particular interest in creep studies since it can be related to the creep mechanism. Theoretically, creep by dislocation climb should yield a stress exponent of about 5,[19] whereas Nabarro-Herring creep[20,21] results in a linear stress dependence. Creep by grain boundary sliding is conventionally thought to result also in a linear relationship between creep rate and stress. Recently, however, Langdon[22] pointed out that reported examples of a linear relationship between $\dot{\epsilon}_{GBS}$ (creep rate due to grain boundary sliding) and σ are restricted to very low stress conditions and that, consequently, models which treat sliding as a Newtonian viscous phenomenon appear incapable of accounting for data obtained under the usual conditions of high temperature creep. Langdon proposed a grain boundary sliding model in which sliding occurs by the movement of dislocations along, or adjacent to, the boundary by a combination of glide and climb, and in which the strain rate due to sliding is proportional to σ^2/d, where d is the average grain diameter. Thus, the theoretical stress exponent for this mechanism is close to the experimental value for creep in (U, Pu)C determined in the present investigation, and is also close to the literature values for creep in UC.[3-5]

It should be noted, however, that whereas the overall stress exponent resulting from a fit of all the secondary creep rate data to Eq. (1) was 2.44, the data points in Fig. 4 could be connected by two sets of straight lines instead of one; one set of lines could connect the 2000 psi and 4000 psi points and another set could connect the 4000 psi and 6000 psi points, thereby yielding two stress exponents, a value of about two for the low stresses and a value greater than three for the higher stress region. This would, therefore, correspond to a change in creep mechanism, possibly from grain boundary sliding to dislocation climb or even glide. Since

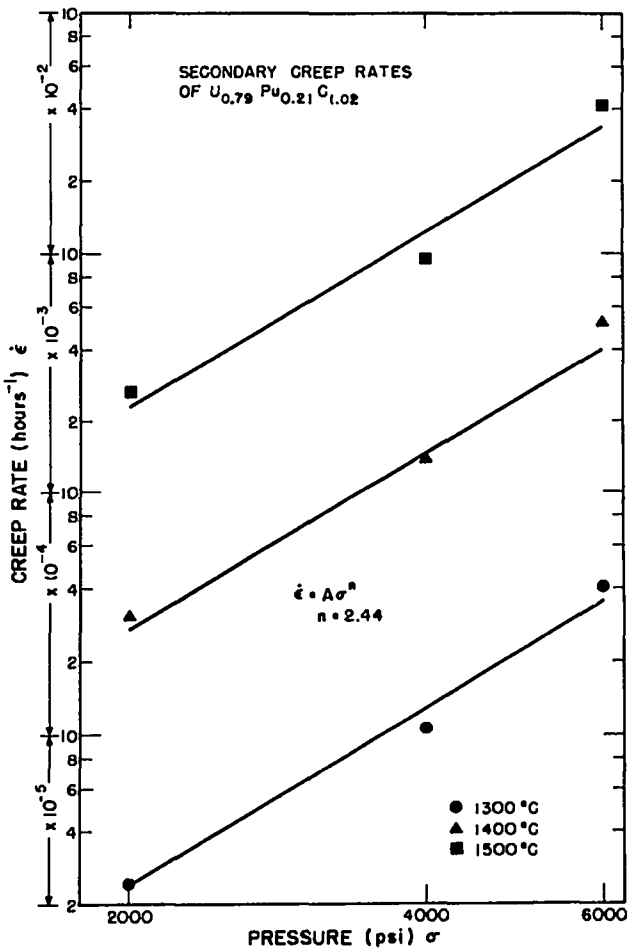

Fig. 4. $\ln \dot{\epsilon}$ vs $\ln \sigma$.

only three stresses were used in this investigation, however, it might be premature to interpret the data in this fashion. Further work performed over a wider stress range is needed to establish whether a change in creep mechanism does occur at high stresses.

Ceramographic studies of crept $U_{0.79}Pu_{0.21}C_{1.02}$ specimens support the indication that grain boundary sliding may be a major creep mechanism in (U, Pu) C. A quantitative evaluation of the amount of grain boundary sliding can be made from measurements of the average grain shape, defined in terms of the parameter (L/B) where L is the average grain length and B is the width, relative to the compressive stress direction.[23,24] Assuming an initial value for L/B of unity (equiaxed grains), the grain strain, i.e. deformation within the grains due to slip or dislocation climb, is

$$\dot{\epsilon}_g = (L/B)^{2/3} - 1. \qquad (3)$$

The relative contributions of the two processes, grain strain and grain boundary sliding, to the overall specimen deformation can be obtained from the ratio of grain strain to total strain, ϵ_g/ϵ_T. If the deformation is due only to straining of the grains, then $\epsilon_g/\epsilon_T = 1$, but if the deformation is due only to relative translational movements of the grain with no change in the average grain shape having taken place, then ϵ_g/ϵ_T is zero.

Taking as an example a $U_{0.79}Pu_{0.21}C_{1.02}$ specimen deformed 25.6% (at 1400°C, 4000 psi), the L/B was determined to be 0.99. Hence, from Eq. (3), the grain strain was practically zero, indicating that almost all the creep strain resulted from grain boundary sliding.

In another example, a specimen deformed 50.6% (at 1500°C, 6000 psi) had an L/B of 0.86, from which ϵ_g was calculated to be 0.10. Thus grain boundary sliding accounted for about 80% ($\epsilon_g/\epsilon_T = 0.10/0.51$) of the deformation in this heavily deformed specimen. Photomicrographs of the specimen after testing and an as-sintered specimen for comparison are shown in Fig. 5. The deformed specimen was sectioned longitudinally to provide a view of a cross section parallel to the compressive stress direction. It should be noted that there is no evidence of severe grain growth in the deformed specimen. Although this does not completely refute the possibility of recrystallization, because the presence of porosity could result in the growth of new grains being stopped at the original size by the distributed pores, the observed constant grain size in this specimen and in specimens crept under different stresses and temperatures are strong evidence for the absence of recrystallization. Nucleation and growth of new grains at different temperatures and stresses would result in a detectable difference in grain size between specimens. Furthermore, no discontinuities were observed in the creep versus strain curves, whereas Hardwick et al[25] reported such discontinuities when recrystallization occurred.

In the literature on grain boundary sliding, some writers[26,27] have suggested that sliding accounts for all of the initial deformation until some "critical" strain when slip first occurs. In some materials, however, it has been found that the creep mechanism depends on the strain rate and temperature. For example, Rachinger[23] reported that at low strain rates and at relatively low temperatures ($\lesssim 200^{\circ}$C) the main contribution to the strain in aluminum is grain strain, whereas above 250°C, relative translational grain movements account for the greater part of deformation, unless the strain rate is high, in which case grain strain accounted for the specimen deformation. For the $U_{0.79}Pu_{0.21}C_{1.02}$ specimen deformed 50.6%, therefore, it is not known at this point whether the grain strain resulted from the high strain rate encountered at the extreme test conditions (1500°C, 6000 psi) or whether the creep mechanism changed at some "critical" strain (or stress). One way to attempt to resolve this question would be to systematically strain a number of specimens at different strain rates to the same total strain, at which point the specimens would be examined ceramographically for grain strain. The effect of temperature would also have to be accounted for, since the creep mechanism could change with temperature.

The interpretation that grain boundary sliding is a major creep mechanism in (U, Pu) C is supported by ceramographic examinations of pore shape. As shown in Fig. 6, pores in an as-sintered pellet are generally rounded and non-oriented, whereas pores in a severely

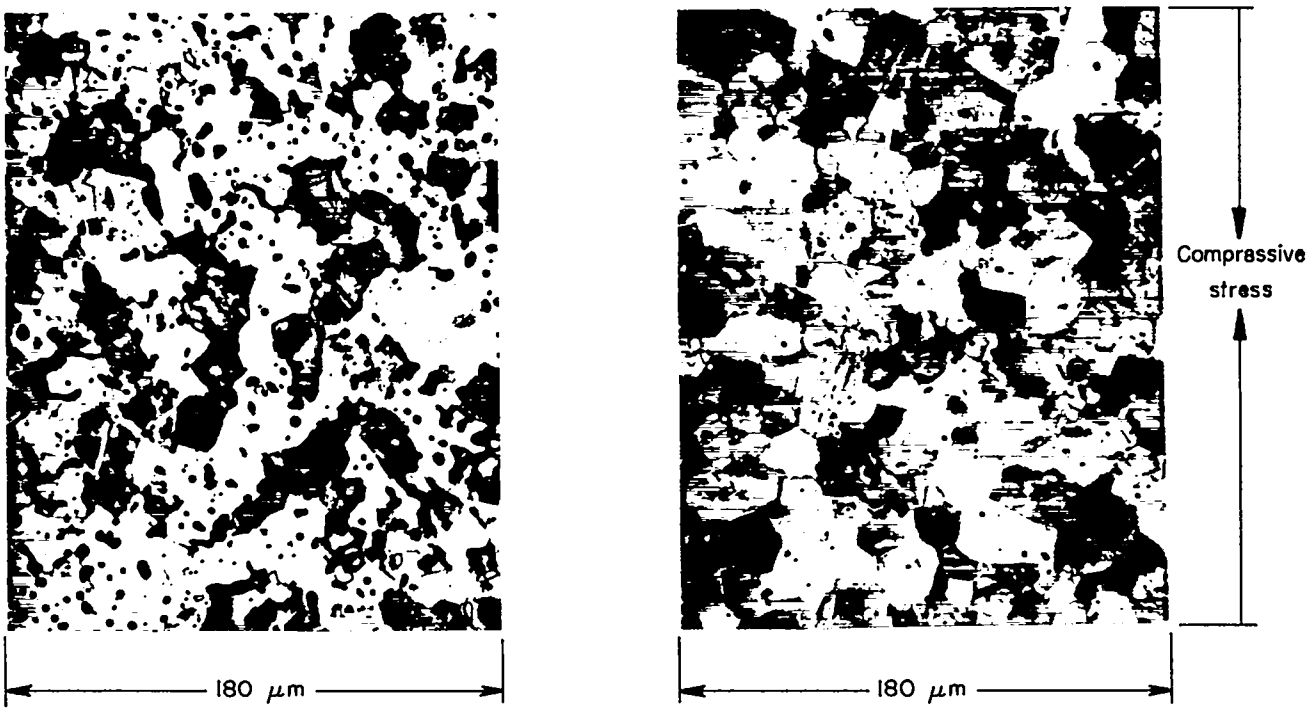

As sintered

Etchant, HNO_3

Creep tested at 1500°C, 6000psi

Total strain = 50.6%

Grain strain ~10%

Fig. 5. Photomicrographs of grain shape.

deformed specimen are elongated and aligned in a direction parallel to the compressive stress direction. This would be the expected configuration in grain boundary pores lying between grains which are sliding by one another; plastic flow would, in contrast, tend to flatten the pores in the compressive stress direction. Of course, grain boundary sliding cannot contribute to deformation indefinitely without auxilliary processes, because some intragranular deformation is necessary to maintain geometrical continuity between the grains. In a specimen which is porous initially, however, changes in pore shape could facilitate sliding by alleviating the grain strain requirement.

It is interesting to note that Stellrecht, et al.[5] obtained evidence of extensive grain strain in creep in UC, but their UC was arc-cast material with a grain size of about 200 to 300 μm, compared to 20 to 30 μm for the sintered (U, Pu)C used in this study. It seems reasonable that grain boundary sliding would be more important in the material which has the larger number of sliding interfaces. Thus there may be some critical grain size below which grain boundary sliding is the predominant creep mechanism and above which dislocation climb is of major importance.

It is hoped that the effects of grain size and porosity on creep rate and mechanism can be determined in future work. If creep rate is found to be inversely proportional to grain size, then Langdon's grain boundary theory would gain further support and the importance of grain boundary sliding in creep of (U, Pu)C would appear to be firmly established. It must be emphasized that the effect of microstructure on creep in the actinide carbides has never been systematically studied, so the mechanisms of mechanical behavior in the materials are still a matter of conjecture.

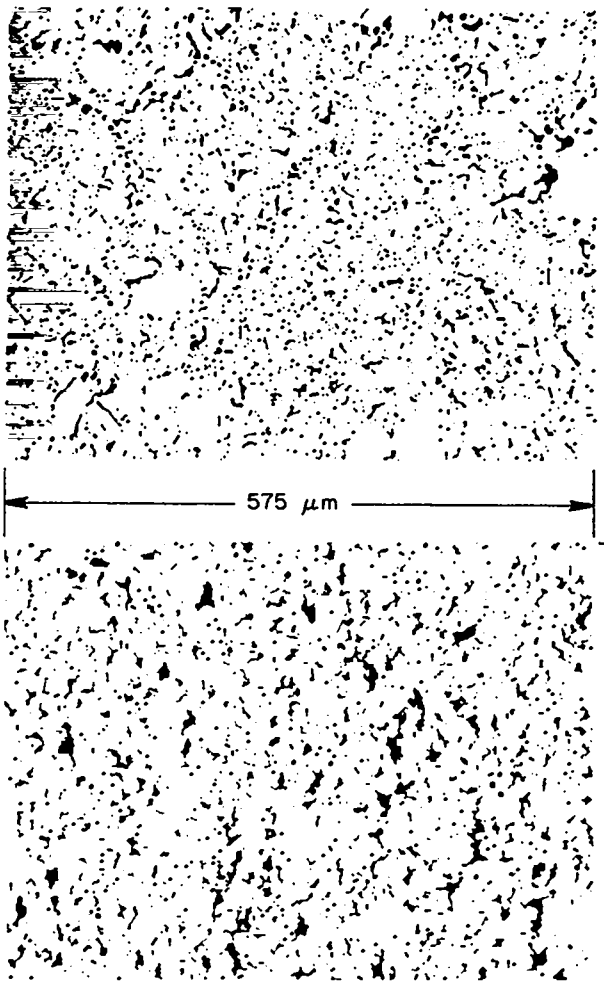

As sintered $U_{0.79}Pu_{0.21}C_{1.02}$ with randomly oriented pores. (As polished)

Longitudinal cross section of $U_{0.79}Pu_{0.21}C_{1.02}$. Creep tested at 1500°C, 2000 psi. Total deformation 33.6%. Pores with serrated edges are aligned in compressive stress direction. (As polished)

Fig. 6. Photomicrographs of pore shape.

III. HOT HARDNESS

A. Equipment and Procedure

A schematic diagram of a hot-hardness tester in use at the LASL plutonium facility is shown in Fig. 7. In this apparatus, the specimen rests on an anvil that can be raised or lowered manually from outside the glovebox by a push-rod which passes through a vacuum gland and water-cooled jacket below the glovebox and furnace chamber bottom plate. The tip of a sheathed platinum-platinum, 10% rhodium thermocouple, inside the hollow push-rod, rests against the underside of the tantalum anvil just below the test specimen. The temperature readings from this thermocouple and another thermocouple positioned between the heating element and the innermost radiation shield are plotted continuously on a two-pen chart recorder.

To make a micro-indentation, the specimen is raised until it contacts the indentor and lifts it off its support. At this instant, the electrical contacts at the indentor support are broken. This provides a means of determining indentation time. A traverse may be made across the specimen by rotating the table below the vacuum chamber; this rotates the anvil. Specimens up to 1-1/2 in. in diameter and of any thickness compatible with ceramographic preparation techniques may be tested. Specimens of small dimensions or odd shapes can be

handled through the use of appropriate mounting jigs. The tests are normally conducted in a vacuum of about 1×10^{-6} Torr (usual vacuum at 1000°C is about 5×10^{-7} Torr). A test load of approximately 200 grams is normally used, although larger loads can be used by adding weights on top of the indentor rod. The hardness numbers are calculated from the standard formula for a Vickers diamond pyramid indentor.

With this type of hardness tester the indentations cannot be measured in situ since there is no viewing system. After the indentations are made and the specimen cooled to room temperature, it is transferred from the plutonium-contaminated glovebox to a standard Leitz microhardness tester-microscope where the indentations are measured. Because of the alpha contamination problem, loose particles are removed from the specimen by washing it in Vythene in an ultrasonic cleaner. Immediately after the washing, the specimen is transferred out of the glovebox to a clean, disposable glass plate. Through this procedure, the spreading of contamination outside the glovebox is avoided.

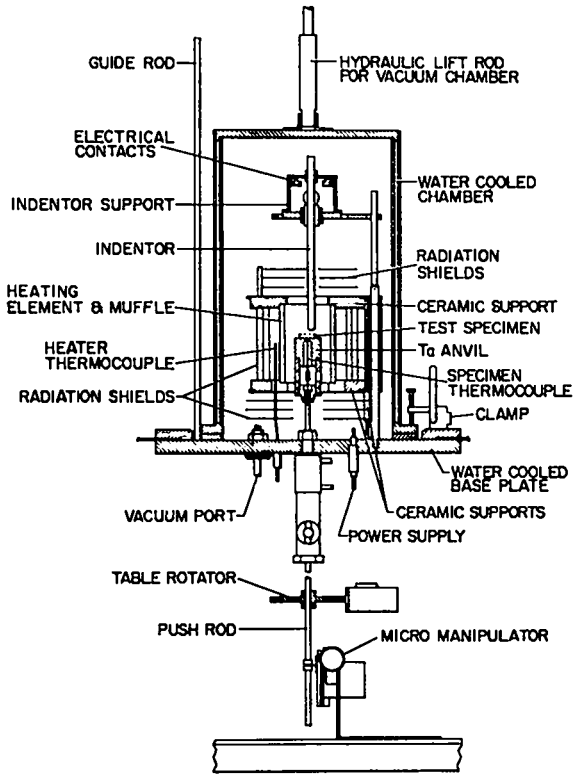

Fig. 7. Hot hardness schematic.

The selection of a suitable indentor material has proven to be a problem. Conventional indentor materials such as sapphire and diamond cannot be used above approximately 1000°C. The sapphire is limited by chemical incompatibility with the carbides, and diamond begins to graphitize at around 1000°C. For temperatures above 1000°C, therefore, B_4C indentors are used. B_4C was chosen as an indentor material because it reportedly retains its high hardness at high temperatures,[28] and it has been used successfully to indent various refractory metal carbides to 1800°C.[29] B_4C indentors have now been used to indent uranium-plutonium carbides to 1200°C. Indentor life at 1200°C is relatively short, apparently due to the fact that the U-Pu monocarbides have a high affinity for carbon. B_4C indentors appear to be attacked particularly severely by monocarbide specimens of substoichiometric composition or high Pu content. A means of readily refurbishing the indentor tips has been developed. The compatibility of other indentor materials is being investigated.

B. Hot Hardness Results and Discussion

Hot hardness curves for various sintered uranium-plutonium carbide compositions are shown in Fig. 8. Each point represents the mean value of 5 to 15 readings taken over 1 to 4 runs. The shapes of the curves are of a similar pattern. The hardness decreases gradually up to about 400-500°C, there is then an increase in softening rate, after which the materials again soften less rapidly with temperature.

In the case of pure metals, plots of log hardness versus temperature have a rather distinctive shape, i.e., two straight line segments intersecting at a temperature near half the melting point ($0.5\ T_m$).[30] Hardness plots for certain intermetallic compounds have been found to have the same shape, but the point of intersection seems to vary between 0.4 and $0.75\ T_m$.[31] The intersecting-straight line form of the log hardness versus temperature plots may be represented by the so-called Ito-Shishshokin[32,33] equation

$$H = A\ e^{-BT} \qquad (4)$$

where H is the hardness, A is a constant, B is the "softening coefficient," and T is the temperature. The constants A and B have one set of values at low temperatures and another set at high temperatures. For the low temperature branch of the log H versus T plot the constant, A, has been regarded as the "intrinsic hardness," i.e., the extrapolated hardness at absolute zero. It is commonly believed that different mechanisms of deformation are operative above and below the intersection temperature; below this temperature slip processes predominate while above this temperature diffusion-controlled processes such as dislocation climb and grain boundary sliding prevail.

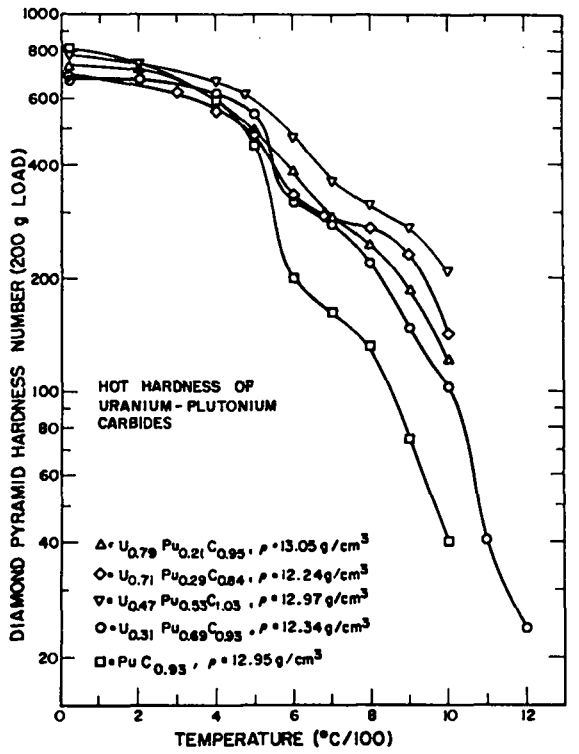

Fig. 8. Hot hardness curves.

A plot of some of the hardness data as a function of homologous temperature (melting point fraction) is shown in Fig. 9. For the solid solution carbides, which melt over a temperature range, solidus temperatures were arbitrarily used as a basis for calculating the homologous temperature or T/T_m. It is apparent that except for the PuC sample, none of the measurements were made at temperatures where high temperature deformation processes are clearly operative, i.e., at temperatures significantly greater than 0.5 T_m. While at temperatures below 0.5 T_m the Ito-Shishshokin relationship is not followed in these materials, sufficient data are not yet available at temperatures above 0.5 T_m to allow a conclusion to be made regarding the applicability of this relationship at high temperatures. An effort is being made to obtain more high temperature data, since it is at these temperatures that the mechanisms for both creep and indentation hardness deformation should be the same (if the differences in type of loading and strain rate prove to have a negligible effect on the deformation mechanism).

At temperatures below 0.5 T_m the non-linearity of the log hardness versus temperature plots is possibly the result of dislocation-impurity (or dislocation-solute)

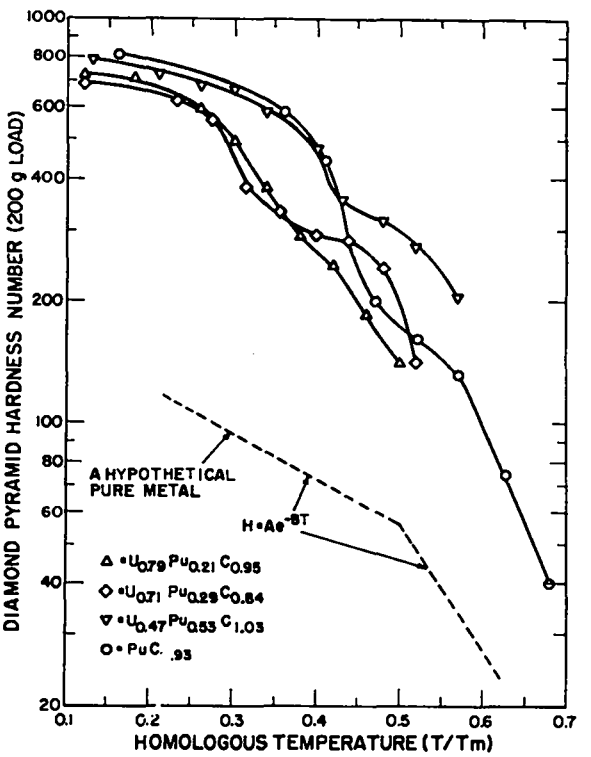

Fig. 9. Hardness vs homologous temperature.

interactions. The relatively slow decrease in hardness with increasing temperature from room temperature to a few hundred degrees centigrade (0.25 to 0.35 T_m) is most likely due to the gradual easing of dislocation glide as a result of the increase in thermal energy of the atoms. The sudden increase in softening rate at slightly higher temperatures might be due to the unpinning of dislocations from impurity atoms which start to diffuse through the lattice, or it could be attributed to the onset of dislocation generation activated by stress and thermal energy. The latter explanation seems more reasonable in view of the observed decrease in softening rate at approximately 0.35 to 0.45 T_m, because dislocation movement could be hampered by impurity species in this higher temperature range. Harrison and Pape[34] have, for example, reported minimum temperatures for diffusion and thermal dislocation generation of 0.33 T_m and 0.30 T_m respectively in UN. Unfortunately these interpretations of the hardness variation with temperature must remain speculative until direct observations of dislocation-impurity interactions can be obtained. This does not appear likely to happen soon due to the difficulty encountered in the preparation of the oxidation-free thin sections required for transmission electron microscopy.

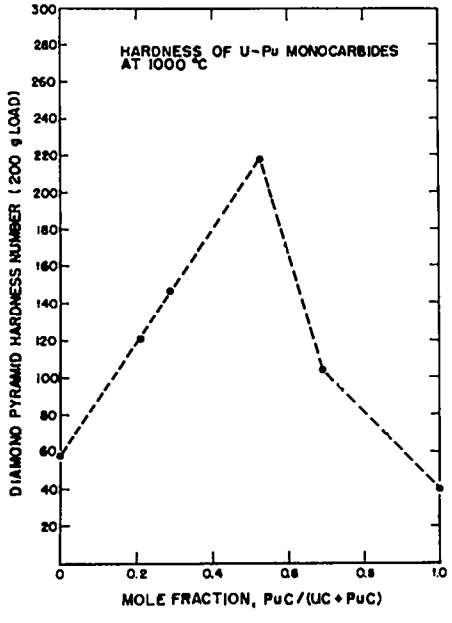

Fig. 10. Hardness vs Pu/U + Pu at 1000°C.

That some solid solution hardening is obtainod from the alloying of UC with PuC is evident from Fig. 10. Although the composition survey is incomplete, it appears that the solid solution carbides were significantly harder than UC at 1000°C (the UC hardness value was taken from the work of DeCrescente and Miller[35]). If this pattern held at higher temperatures, solid solution carbides would be expected to be more creep resistant than UC, yet as shown in Fig. 11, the (U, Pu)C creep tested in this study had higher creep rates than reported for UC by Stellrecht et al.[5] If one were to extrapolate the creep data to lower temperatures, however, he would find that at about 1050°C the lines would cross, i.e., the creep rate of UC would be equal to that of the solid solution carbide.

A possible explanation for this apparent anomaly lies in the theory of solid solution strengthening. At very high temperatures the deformation mechanism is almost certainly diffusion-controlled, but if in (U, Pu)C the diffusivity of the solute Pu ions is sufficiently high,

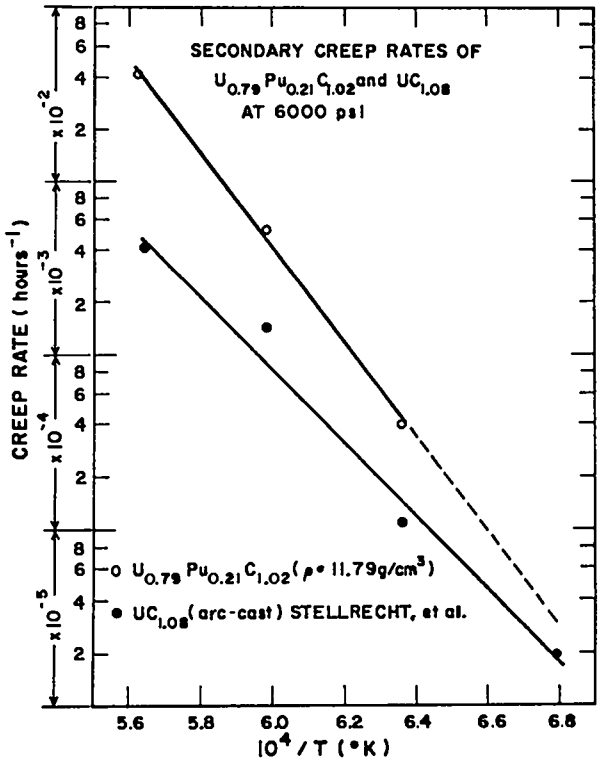

Fig. 11. Creep of (U, Pu)C and UC.

there may be no "impurity" retardation of dislocation motion. At intermediate temperatures, however, (that is, at temperatures near 0.5 T_m) the drift velocity of the solute atoms might be expected to decrease to a point such that the moving dislocations are, in effect, pulled back, yielding a higher hardness than that obtained for pure UC. As mentioned earlier, self-diffusion data for Pu in the solid-solution carbides are not available, and this theory remains unsupported by independent property measurements, but in Al-Mg alloys[36] and in UC_{1+x}[2] similar dislocation-impurity interactions have been held responsible for anomalous peaks in creep activation energy versus temperature curves.

The complex nature of the bonding in the U-Pu carbides is such that comparison of their hardness measurements with those of other ceramics is of limited value. The reader is referred to a paper by Westbrook[37] for a general comparison of the high temperature hardness of some carbides with the NaCl structure with other materials of similar structure. In spite of the fact that indentation hardness involves a complicated state of stress, hardness values have been found to bear a relationship to several mechanical and atomic properties such as yield point, tensile strength, fatigue strength, creep, crystal structure, compressibility, and ionic radii; and have even been correlated with certain electrical, magnetic, and thermodynamic properties.[38-41] It may be possible, therefore, to obtain a correlation between hot hardness and creep for the U-Pu carbides. Such correlations have been found for various steels of even more complex composition and microstructure[41] than encountered in the actinide carbides.

IV. SUMMARY

Compressive creep studies have been made on uranium-plutonium carbides, having the composition $U_{0.79}Pu_{0.21}C_{1.02}$. While creep rates in the (U, Pu)C tested in this investigation were higher than have been reported for UC tested under similar conditions, this may be, at least partially, the result of differences in porosity and grain size in the two materials. More work is required to establish quantitatively the effects of grain size and porosity on mechanical properties of the U-Pu carbides.

The creep and hardness measurements have yielded information on possible deformation mechanisms in the uranium-plutonium carbides. The relative contributions of these mechanisms apparently changes with temperature and microstructure and may also change with strain rate. Undoubtedly the slow progress that has been made in uncovering the basic mechanisms of deformation must be attributable to the inherent complexity of the crystallographic processes that control the mechanical properties. It is hoped that the results obtained here will provide in part the necessary pattern for formulating the laws of deformation from which engineering properties may be predicted.

ACKNOWLEDGMENTS

The author is indebted to R. E. Honnell, R. W. Walker, H. G. Moore, and W. Hayes for specimen preparation; to K. A. Johnson and C. Baker for ceramographic preparation, and to Dr. C. F. Metz and the analytical group for chemical analyses. Special thanks should go to Dr. J. L. Green for criticizing the manuscript.

REFERENCES

1. C. H. de Novion, B. Amice, A. Groff, Y. Guerin, and A. Padel, "Mechanical Properties of Uranium and Plutonium-Based Ceramics," Plutonium 1970 and Other Actinides, Part 1, W. N. Miner, Ed., (1970) pp. 509-515.

2. N. M. Killey, E. King, and H. J. Hedger, "Creep of U and (U, Pu) Monocarbides in Compression," AERE-R 6486 (1970).

3. J. J. Norreys, "The Compressive-Creep of Uranium Monocarbide," in Carbides in Nuclear Energy, Vol. 1, L. E. Russel, Ed., Macmillan and Co. Ltd., London, 1964, pp. 435-446.

4. M. H. Fassler, F. J. Heugel, and M. A. DeCrescente, "Compressive Creep of UC and UN," PWAC-482, Part 1, October 1965.

5. D. E. Stellrecht, M. S. Farkas, and D. P. Moak, "Compressive Creep in Uranium Carbide," J. Am. Ceram. Soc. 51, 455-458 (1968).

6. R. Chang, "The Flow and Recovery Properties of Nearly Stoichiometric Polycrystalline Uranium Carbide and Mechanism of Work Hardening of Crystalline Solids," NAA-SR-6481, March 1962.

7. P. Magnier, M. Marchal, and A. Accary, "High Temperature Compressive Creep and Hot Extrusion of Uranium-Carbon Alloys," Proc. Brit. Ceram. Soc. 7, 141-158 (1967).

8. D. E. Stellrecht, D. E. Price, and D. P. Moak, "Creep Rupture of High Temperature Fuels," BMI-1859, Feb. 1969.

9. A. Accary, P. Magnier, and M. Marchal, "Mechanical Behavior of Uranium Carbon Alloys Close to UC and Their Fabrication by Extrusion," Rev. Hautes Temp. et Refractaires 3, 59-77 (1966).

10. G. G. Bentle and G. Ervin, "Self-Diffusion of Uranium and Carbon in Uranium Monocarbide," AI-AEC-12726, August 1968.

11. R. A. Kratkowski, "Self-Diffusion of Carbon in Uranium Monocarbide," J. Nucl. Mater. 32, 120-125 (1969).

12. T. C. Wallace, W. G. Witteman, C. L. Radosavich, and M. G. Bowman, "Carbon Diffusion in the Carbides of Uranium," in High Temperature Materials, Papers presented at the Sixth Plansee Seminar, June 24-28, 1968, Reutte, (F. Benesovsky, ed.) pp. 676-700, Springer-Varlag, Wien and New York.

13. R. Lindner, G. Riemer, and H. L. Scharff, "Self-Diffusion of Uranium in UC," J. Nucl. Mater. 23, 222-230 (1967).

14. W. Chubb, C. W. Townley, and R. W. Getz, "Diffusion in Uranium Monocarbide," J. Nucl. Mater. 13, 63 (1964).

15. (a) P. Villaine and J. F. Marin, "Autoradiographic Evidence for Intergranular Diffusion of U in UC," Compt. rend. 262c, 1660 (1966).
(b) "Self-Diffusion Coefficient of Uranium in Uranium Monocarbide," Compt. rend. 264c, 2015 (1967).

16. H. M. Lee and L. R. Barrett, "Measurements of Self-Diffusion in Uranium Carbides and Their Application to Related Activated Processes," Proc. Brit. Ceram. Soc. 7, 159-176 (1967).

17. A. Accary and J. Trouve, Mem. Scient. Rev. Met. 60, 117 (1963).

18. O. D. Sherby and P. M. Burke, "Mechanical Behavior of Crystalline Solids at Elevated Temperatures," in Progress in Materials Science, Vol. 13, B. Chalmers and W. Hume-Rothery, Eds., Pergamon Press, pp. 325-390.

19. J. R. Weertman, "Theory of Steady-State Creep Based on Dislocation Climb," J. Appl. Phys. 26, 1213 (1955).

20. F. R. N. Nabarro, "Deformation of Crystals by Motion of Single Ions," Rept. Conf. Strength of Solids, University of Bristol, 75 (1948).

21. C. Herring, "Diffusional Viscosity of a Polycrystalline Solid," J. Appl. Phys. 21, (5) 437-445 (1950).

22. T. G. Langdon, "Grain Boundary Sliding as a Deformation Mechanism During Creep," Phil. Mag. 22, 689-700 (1970).

23. W. A. Rachinger, "Relative Grain Translations in the Plastic Flow of Aluminum," J. Inst. of Metals 81, 33-41 (1952-53).

24. J. H. Hensler and R. C. Gifkins, "The Estimation of Slip Strain During Creep," J. Inst. Metals 92, 340 (1963-64).

25. D. Hardwick, C. M. Sellars, and W. J. McG. Tegart, "Occurrence of Recrystallization During High-Temperature Creep," J. Inst. Metals 90 (1) 21-22 (1961-62).

26. V. S. Ivanova, Dokl. Akad. Nauk. U. S. S. R. 94 (2) 217 (1954).

27. Ya. R. Rauzin and A. R. Zhelezniakova, Fiz, Met. Metallov. 3, 146 (1956).

28. L. M. Fitzgerald, "The Hardness at High Temperatures of Some Refractory Carbides and Borides," J. Less Common Metals 5, 356-364 (1963).

29. R. D. Koester and D. P. Moak, "Hot Hardness Indentors for Temperatures Approaching 2000°C," J. Less Common Metals 13, 249-252 (1967).

30. J. H. Westbrook, "Temperature Dependence of the Hardness of Pure Metals," Trans. Amer. Soc. Metals 45, 221-248 (1953).

31. E. R. Petty, "Hot Hardness and Other Properties of Some Binary Intermetallic Compounds of Aluminum," J. Inst. Metals 89, 343-349 (1960).

32. K. Ito, "The Hardness of Metals as Affected by Temperature," Tohoku Science Repts. 12, 137 (1923).

33. V. P. Shishshokin, "The Hardness and Fluidity of Metals at Different Temperatures," Zeitschrift für Physikalische Chemie 189, 263 (1930).

34. J. D. Harrison and R. P. Pape, "Factors Affecting the Hardness of Uranium Mononitride," Plutonium 1970 and Other Actinides, Part 1, 518-525 (1970).

35. M.A. DeCrescente and A.D. Miller, "High Temperature Properties of Uranium Carbide," in Carbides in Nuclear Energy, L.E. Russel, Ed., Macmillan and Co. Ltd., London, 342-357 (1964).

36. N.R. Borch, L.A. Shepard, and J.E. Dorn, Trans. A.S.M. 52, 494 (1960).

37. J.H. Westbrook, "The Temperature Dependence of Hardness of Some Common Oxides," Rev. Hautes Temp. et Refractaires 3, 47-57 (1966).

38. E.R. Petty and H. O'Neill, "Hot Hardness Values in Relation to the Physical Properties of Metals," Metallurgia 60, 25-30 (1961).

39. E.R. Petty, "Hardness and Other Physical Properties of Metals in Relation to Temperature," Metallurgia 56, 231-235 (1957).

40. S.F. Pugh, "Relations Between the Elastic Moduli and the Plastic Properties of Polycrystalline Pure Metals," Phil. Mag. 45, 823-834 (1954).

41. F. Garofalo, P.R. Malenock, and G.V. Smith, "Hardness of Various Steels at Elevated Temperatures," Trans. Amer. Soc. Metals 45, 377-396 (1952).